Data-driven Modeling of Reflection Point Distance Relevant to Diffracting Detonation Wave by Using Machine Learning

Akira Kawasaki[1], Hiroki Hasegawa[1], Han Sun[1], Hiroaki Watanabe[1], Noboru Itouyama[1], Ken Matsuoka[1], Jiro Kasahara[1], Akiko Matsuo[2], Ikkoh Funaki[3]
1 Nagoya University, Nagoya, Aichi, Japan
2 Keio University, Yokohama, Kanagawa, Japan
3 Japan Aerospace Exploration Agency, Sagamihara, Kanagawa, Japan

1 Introduction

Recently, utilization of detonation in aerospace propulsion devices has become increasingly active as a research topic [1–4]. Upon design of those devices, it is essentially important to predict detonation phenomena, such as the detonation limit, the deflagration-to-detonation transition distance, the critical energy for the direct initiation, and the critical diameter for the diffraction. However, fully theoretical prediction is still challenging mainly because of complexity due to essentially time-dependent, three-dimensional nature of the detonation wave [5].

Therefore, characteristic length scales of the detonation wave are often incorporated to utilize some semi-empirical correlations of the detonation dynamics. Although detonation cell width, which is one of the most accepted characteristic length scales, has been measured for various fuel-oxidizer premixtures at various temperatures, pressures, and mixing ratios [6], a wide range of conditions required for the designing are not necessarily covered. Therefore, some researchers are attempting to organize the cell width as a function of thermodynamic and chemical properties [7–10]. Nevertheless, it is still not clear what are suitable properties to predict the cell width.

In this study, we made another attempt to predict a characteristic length scale. In particular, *reflection point distance*, which is acknowledged as a characteristic length scale relevant to the detonation diffraction [11,12], was utilized as the target of the prediction. A data-driven approach was taken for the prediction; namely, functional relationship between the reflection point distance and its potential explanatory variables was acquired statistically based on a lot of experimental data. Artificial neural network (ANN) was particularly employed as the learning model due to its high approximation capability [13]. Objectives are to investigate what the learning process should be and examine the prediction capability of the obtained. Brief overview of this study is described below.

Correspondence to: kawasaki@nuae.nagoya-u.ac.jp

2 Method of Machine Learning

2.1 Dataset

The dataset utilized in this study, part of which is published in References [11] and [14], is shown in Table 1. The reflection point distances were obtained in high-speed imaging experiments of detonation diffraction processes performed by the authors for some fuel-oxidizer premixtures (Fig. 1). At the room temperature, the initial pressure of the mixture was changed successively.

Table 1: Dataset (ϕ: equivalence ratio, X_{dil}: volumetric fraction of diluent)

#	Fuel	Oxidizer	Diluent	ϕ	X_{dil}, %	# of data
1	H_2	O_2	-	0.55–1.30	-	179
2	C_2H_2	O_2	-	0.55–1.30	-	364
3	C_2H_2	O_2	Ar	1.00	50	281
4	C_2H_2	O_2	Ar	1.00	80	15
5	C_2H_2	O_2	N_2	1.00	50	6
6	C_2H_4	O_2	-	0.55–1.60	-	122
7	C_2H_4	O_2	Ar	1.00	50	20
8	C_2H_4	O_2	Ar	1.00	67	47
9	C_2H_4	O_2	Ar	1.00	75	54
10	C_2H_6	O_2	-	0.55–1.39	-	96
11	C_2H_6	N_2O	-	1.00	-	22

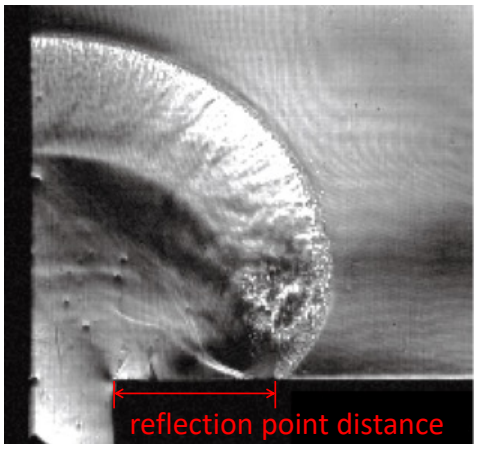

Figure 1: Conceptual definition of the reflection point distance.

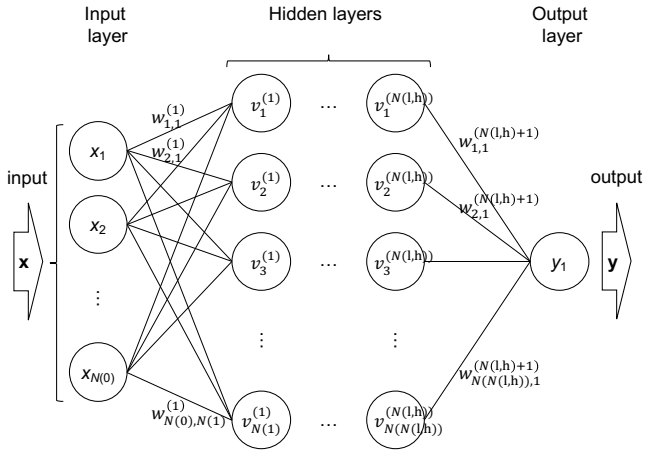

Figure 2: Schematic of a totally coupled multi-layer neural network.

2.2 Learning Model

A schematic of the ANN trained in this study is shown in Fig. 2. The network is the totally coupled type with a layered structure. That is, each neuron (node) j in an hidden layer i takes the value obtained by the affine transformation of the linear combination of the output value $v_{j'}^{(i-1)}$ of node j' in the upstream layer i–1 as the input, and outputs the value $v_j^{(i)}$ obtained through an activation function $\sigma(\cdot)$:$\mathbf{R}\rightarrow\mathbf{R}$.

$$v_j^{(i)} = \sigma\left(z_j^{(i)}\right), \quad z_j^{(i)} = \left[\sum_{j'\in[1,N^{(i-1)}]} w_{j',j}^{(i)} v_{j'}^{(i-1)}\right] + b_j^{(i)}$$

where $w_{(j',j)}^{(i)}$ is the weight of the linear combination, $b_j^{(i)}$ is the bias of the affine transformation, and $\mathbf{R}$ is the set of real numbers. For the activation function, the rectified linear function (ReLU)

$$\sigma(z) = \begin{cases} 0 & (z < 0) \\ z & (z \geq 0) \end{cases}$$

was used.

2.3 Learning Algorithm

The ANN described above can be interpreted as a function $y = f(\boldsymbol{x}; \boldsymbol{\theta})$, that maps an explanatory variable (vector) $\boldsymbol{x}$ to an objective variable y under a parameter (vector) $\boldsymbol{\theta}$, which consist of the weights $w_{(j',j)}^{(i)}$ and the biases $b_j^{(i)}$. For this ANN, if we take a sample ($\boldsymbol{x}_{\mathrm{train},k}$, $y_{\mathrm{train},k}$) from the training dataset, we get a prediction of the objective variable, $y_{\mathrm{pred},k}$, under the explanatory variables $x_{\mathrm{train},k}$ and a certain $\boldsymbol{\theta}$. By comparing the predicted data $y_{\mathrm{pred},k}$, with the training data $y_{\mathrm{train},k}$, the loss function

$$\mathrm{Loss}\left(y_{\mathrm{pred},k}, y_{\mathrm{train},k}, \boldsymbol{\theta}\right) = \frac{1}{2}\left\|y_{\mathrm{pred},k} - y_{\mathrm{train},k}\right\|_2^2 + \frac{1}{2}\alpha\|\boldsymbol{w}\|_2^2$$

can be calculated. Here, $\|\cdot\|_2$ is the L2 norm, α is the L2 regularization parameter, and $\boldsymbol{w}$ is a vector consisting of the weights. The second term on the right-hand side is called the regularization term, which has the effect of preventing overfitting of the ANN. Training of the ANN is an optimization problem to minimize the loss function by updating $\boldsymbol{\theta}$. In this study, the stochastic gradient descent (SGD) method was utilized for the updating of $\boldsymbol{\theta}$. To implement this algorithm, we used the scikit-learn [15] programing library.

2.4 Explanatory Variables

In the supervised machine learning, the inputs to the learning model are often called explanatory variables (or features), and the outputs are called objective variables. If initial temperature, pressure, and composition of a mixture are given, the chemical equilibrium calculation can be used to calculate the initial (or pre-shock), von-Neumann (or post-shock), and Chapman-Jouguet (CJ) states. In the training of the ANN, these variables, which were calculated using the NASA CEA code [16], were employed as features. As chemical-kinetics parameters, activation energy, induction length, and reaction length which were computed by using the Cantera [17] and Shock and Detonation Toolbox [18] libraries with the GRI-Mech 3.0 [19] chemical-kinetics mechanism, were also employed as features. In this way, the chemical species, which are not numerical but categorical variables, were characterized by numerical variables.

Since strong correlations between features can degrade the accountability of the learned model, features strongly correlate with other features were excluded. The strength of correlation was measured based on Spearman's rank-correlation coefficient, and threshold was set to 0.9. As a result,

$$\boldsymbol{x} = \left(T_0, p_0, \rho_0, h_0, g_0, \bar{M}_0, \gamma_0, T_{\mathrm{vN}}, u_{\mathrm{vN}}, a_{\mathrm{vN}}, Pr_{\mathrm{vN}}, T_{\mathrm{CJ}}, \bar{M}_{\mathrm{CJ}}, Pr_{\mathrm{CJ}}, D_{\mathrm{det}}, M_{\mathrm{det}}, E_{\mathrm{a}}, \Delta_{\mathrm{i}}, \Delta_{\mathrm{r}}\right)^T$$

were selected as the input parameters of the model. Here, T is temperature, p is pressure, ρ is specific enthalpy, u is specific internal energy, h is specific enthalpy, g is specific Gibbs free energy, $\bar{M}$ is molecular mass, a is speed of sound, γ is specific heat ratio, Pr is Prandtl number, D_{det} is the CJ detonation velocity, M_{det} is the CJ detonation Mach number, E_{a} is the activation energy, Δ_{i} is the induction length, and Δ_{r} is the reaction length. The subscripts are as follows: 0 is the initial (pre-shock) state, vN is the von Neumann (post-shock) state, and CJ is the CJ state.

3 Results and Discussion

3.1 Model Optimization Results

The number of the layers $N_{l,h}$, the number of the nodes par layer $N_{n,h}$, and the regularization parameter α were optimized by cross validation. As a result, $N_{l,h}$, $N_{n,h}$, and α were set to 6, 300, and 10^{-2}, respectively. The coefficient of determination

$$R^2(\boldsymbol{y}_{\text{pred}}, \boldsymbol{y}_{\text{train}}) = 1 - \frac{\sum_k (y_{\text{train},k} - y_{\text{pred},k})^2}{\sum_k (y_{\text{train},k} - \bar{y}_{\text{train}})^2}$$

was used as the scoring parameter to evaluate the model performance. A value closer to unity means the smaller difference between the predicted values by the trained model and the experimental data for validation. As a result of the optimization, a mean R^2 value of 0.960 was attained. In the following, we will only discuss the results for the optimized model.

3.2 Regression Performance

Figure 3 shows relationship between each output (predicted reflection point distance) by the trained model $f(\cdot\,; \boldsymbol{\theta}_{\text{trained}})$ when the corresponding feature vector $\boldsymbol{x}_k$ used in the training is input

$$\boldsymbol{l}_{\text{r,pred},k} = \boldsymbol{y}_{\text{pred},k} = \boldsymbol{f}(\boldsymbol{x}_k; \boldsymbol{\theta}_{\text{trained}})$$

and the corresponding training datum (experimental reflection point distance) $l_{\text{r,exp},k} = y_{\text{train},k}$. The red line in the figure shows the line of exact agreement between the model predictions and experimental values. As shown in the figure, the predictions of the trained model are in good agreement with the experimental data. This indicates that the trained model was well fitted (regressed) to the training data.

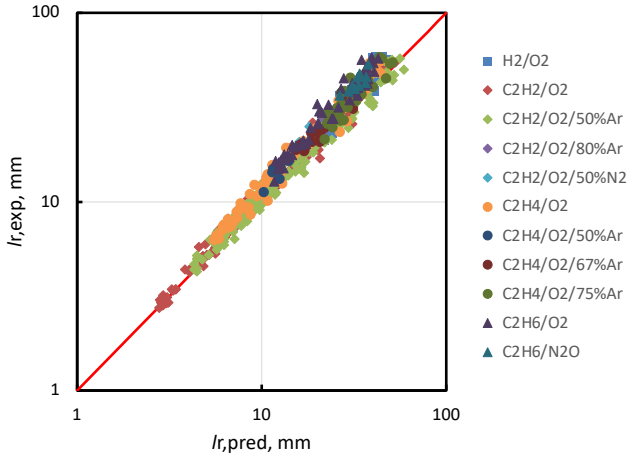

Figure 3: Relationship between experimental data, $l_{\text{r,exp}}$, and model predictions, $l_{\text{r,pred}}$, for the training data.

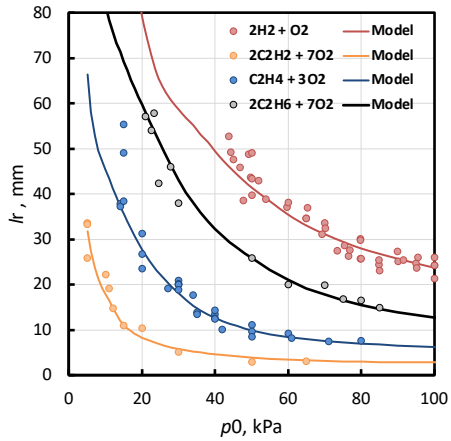

Figure 4: Model dependence on initial pressure.

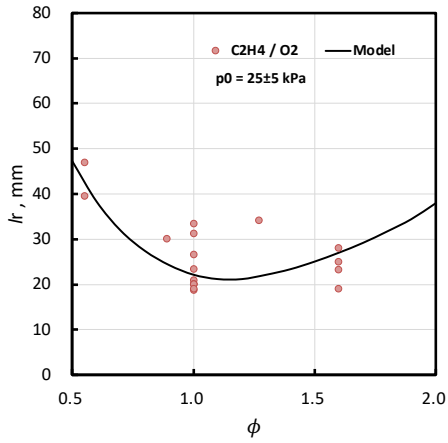

Figure 5: Model dependence on equivalence ratio.

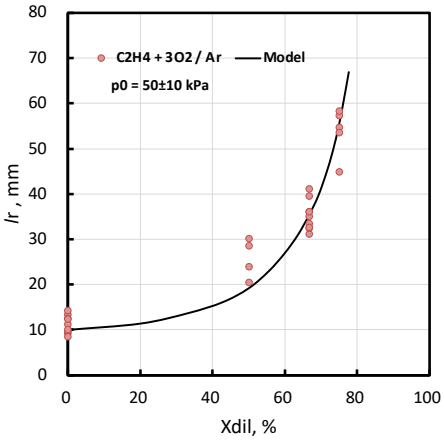

Figure 6: Model dependence on dilution ratio.

The regression performance is further examined for some reaction systems. Figures 4–6 show typical behavior of the trained model when the initial pressure, equivalence ratio, and dilution ratio were changed. As shown in Figure 4, the trained model well acquired appropriate behavior for the change in the initial pressure. As shown in Figures 5 and 6, the trained model also well acquired appropriate behavior for the equivalence ratio and dilution ratio of the reactants.

3.3 Prediction Performance

Figure 7 shows relationship between each predicted reflection point distance by the trained model

$$\boldsymbol{l}_{\mathbf{r,pred},k'} = \mathbf{y}_{\mathbf{pred},k'} = \boldsymbol{f}(\boldsymbol{x}_{k'}; \boldsymbol{\theta}_{\mathbf{trained}})$$

and the corresponding experimental value $l_{\mathrm{r,exp},k'} = y_{\mathrm{train},k'}$ for the test data, which are not used for the training of the model and extracted at random from Table 1. The red line in the figure shows the line of exact agreement between the model predictions and experimental data. As shown in the figure, the predictions of the trained model are in good agreement with the experimental values even for the data that are not used for the training. This suggests that the trained model has good prediction capability for unknown experimental data; that is, the model is well generalized.

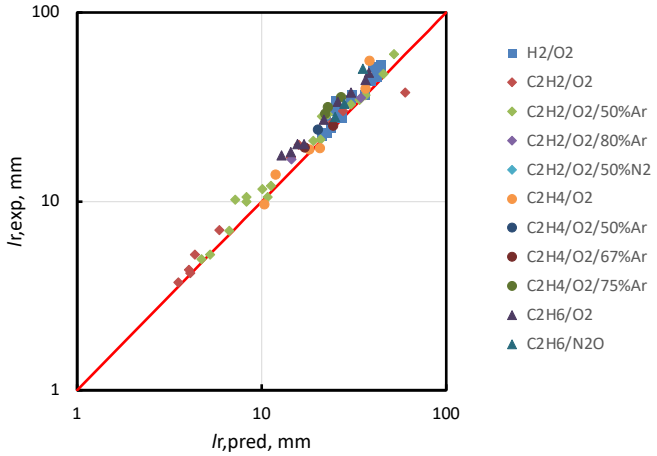

Figure 7: Relationship between experimental data, $l_{\mathrm{r,exp}}$, and model predictions, $l_{\mathrm{r,pred}}$, for the test data.

4 Conclusions

In this study, a predictive model of the reflection point distance, which is a characteristic length scale relevant to detonation diffraction, was constructed and evaluated based on an existing experimental dataset for familiar gaseous fuels, including hydrogen (H_2), acetylene (C_2H_2), ethylene (C_2H_4), and ethane (C_2H_6). The model was a statistical model obtained by a data-driven approach utilizing methods of machine learning, in which the reflection point distance was a function of thermodynamic and chemical parameters of fuel-oxidizer mixtures. A multilayer, totally coupled neural network was particularly chosen as the (abstract) learning model. As a result, we obtained the following conclusions.

- The obtained model exhibits a good regression performance. That is, the model well acquired typical dependencies of the reflection point distance on the initial pressure, equivalence ratio, and dilution ratio.
- The obtained model also exhibits a good prediction performance. That is, the model well predicted reflection point distances unknown for the model. This suggests that the model has been well generalized.

References

[1] Kailasanath K. (2000). Review of Propulsion Applications of Detonation Waves. AIAA J. 28: 1698.

[2] Wolanski P. (2013). Detonation propulsion. Proc. Combust. Inst. 34: 125.

[3] Lu FK, Braun EM. (2014). Rotating Detonation Wave Propulsion: Experimental Challenges, Modeling, and Engine Concepts, J. Propul. Power. 30: 1125.

[4] Rankin BA, Kaemming TA, Theuerkauf SW, Schauer FR. (2017). Overview of Performance, Application, and Analysis of Rotating Detonation Engine Technology. J. Propul. Power. 33: 131.

[5] Zhang F. (Ed.) (2012). Shock Wave Science and Technology Reference Library Volume 6 Detonation Dynamics. Springer. (ISBN 978-3-642-22967-1)

[6] Kaneshige M, Shepherd JE. (1997). Detonation database. Technical Report FM97-8, GALCIT.

[7] Gavrikov AI, Efimenko AA, Dorofeev SB (2000). A model for detonation cell size prediction from chemical kinetics. Combust. Flame. 120: 19.

[8] Ng HD, Chao J, Yatsufusa T, Lee JHS. (2009) Measurement and chemical kinetic prediction of detonation sensitivity and cellular structure characteristics in dimethyl ether–oxygen mixtures. Fuel. 88: 124.

[9] Yu JY, Hou BX, Lelyakin A, Xu ZJ, Jordan T. (2017). Gas detonation cell width prediction model based on support vector regression. Nucl. Eng. Tech. 49: 1423.

[10] Malik K, Żbikowski M, Teodorczyk A. (2019). Detonation cell size model based on deep neural network for hydrogen, methane and propane mixtures with air and oxygen. Nucl. Eng. Tech. 51: 424.

[11] Kawasaki A, Kasahara J. (2019). A novel characteristic length of detonation relevant to supercritical diffraction. Shock Waves. 30: 1.

[12] Lee JHS. (1996). On the critical diameter problem. In: Bowen B. (ed.) Dynamics of Exothermicity. (ISBN: 9782884491709)

[13] Cybenko G. (1989). Approximation by superpositions of a sigmoidal function. Math. Control Signal. System. 2: 303.

[14] Sun H, Kawasaki A, Matsuoka K, Kasahara J. (2020). A study on detonation-diffraction reflection point distances in H2/O2, C2H2/O2, and C2H4/O2 systems. Proc. Combust. Inst. 38: 3605.

[15] Pedregosa F, Varoquaux G, Gramfort A, Michel V, Thirion B, Grisel O, Blondel M, Prettenhofer P, Weiss R, Dubourg V, Vanderplas J, Passos A, Cournapeau D, Brucher M, Perrot M, Duchesnay É. (2011). Scikit-learn: Machine Learning in Python. J. Mach. Learn. Res. 12: 2825.

[16] McBride BJ, Gordon S. (1996). Computer Program for Calculation of Complex Chemical Equilibrium Compositions and Applications II. User's Manual and Program Description. NASA RP-1311-P2.

[17] Goodwin DG, Speth RL, Moffat HK, Weber BW. (2021). Cantera: An object-oriented software toolkit for chemical kinetics, thermodynamics, and transport processes. https://www.cantera.org.

[18] Browne S, Ziegler J, Bitter N, Schmidt B, Lawson J, Shepherd JE. (2021).SDToolbox - Numerical Tools for Shock and Detonation Wave Modeling. Explosion Dynamics Laboratory. GALCIT Technical Report FM2018.001. Revised January 2021.

[19] Smith GP, Golden DM, Frenklach M, Moriarty NW, Eiteneer B, Goldenberg M, Bowman CT, Hanson RK, Song S, Gardiner WC, Jr., Lissianski VV, Qin Z. http://www.me.berkeley.edu/gri_mech/